Springer

KSME

Journal of Mechanical Science and Technology 26 (11) (2012) 3411~3422
www.springerlink.com/content/1738-494x
DOI 10.1007/s12206-012-0857-x

A pendulum-like tuned vibration absorber and its application to a multi-mode system †

Xinglong Gong*, Chao Peng, Shouhu Xuan, Yulei Xu and Zhenbang Xu

CAS Key Laboratory of Mechanical Behavior and Design of Materials, Department of Modern Mechanics, University of Science and Technology of China, Hefei 230027, China

(Manuscript Received February 3, 2012; Revised May 7, 2012; Accepted June 28, 2012)

Abstract

This paper presents the design of a pendulum-like adaptive tuned vibration absorber (ATVA) and its application to a multi-mode system. The natural frequency of the pendulum-like ATVA can be adjusted in real time by adjusting its geometric parameters. The principle and the dynamic property of the ATVA are theoretically analyzed. Based on the analysis, a prototype of the ATVA is proposed and developed. Simulations are carried out to predict the effectiveness of the ATVA when applied to the multi-mode system. The simulated results are verified by experimental studies, which are conducted on a multi-mode platform that comprises mass, isolator, and a flexible base. The results indicate that the ATVA installed on an optimized location in the system can effectively reduce vibration over a broad frequency range and can perform better than a tuned vibration absorber.

Keywords: Pendulum-like ATVA; Multi-mode system; Vibration absorber; Vibration attenuation effect

1. Introduction

Tuned vibration absorbers (TVAs), which were invented by Frahm in 1909 [1], have been widely used in suppressing undesired vibrations because of their simple structure and obvious effect in vibration control fields [2-6]. The TVA is a single-frequency vibration control device that only works within a narrow frequency range. If the exciting frequency is in a wide range, the vibration attenuation effect of the TVA often decreases or even collapses because of mistuning [7]. This problem is a major limitation of TVAs in many practical applications. To overcome this defect, an adaptive tuned vibration absorber (ATVA) has been developed [8-10]. The ATVA can expand the effective frequency band and significantly improve its performance in many applications by properly adjusting its natural frequencies in real time to track the exciting frequency. In comparison with the active vibration absorber, the ATVA consumes less power because it does not require active force. Moreover, the ATVA is a fail-safe device because it can work as a TVA in case of power loss.

A number of approaches have been proposed to develop novel ATVAs, including varying the mass distribution by mechanical mechanisms [8, 11], tuning stiffness through mechanical mechanisms [12-17], varying the magnetic spring controlled by current [18], or using controllable new materials [19-21]. The mechanical ATVA, which tunes its natural frequency through mechanical mechanisms, has many advantages. It ensures the stability, durability, and availability of devices. Therefore, this kind of ATVA has been attracting a wide range of interests. Franchek and his colleagues [12] developed an effective ATVA by using a helical spring as the tunable stiffness element, which can be adjusted by varying the effective number of coils. The stiffness of a cantilever beam has been reported to be dependent on its effective length. Therefore, the cantilever beam can serve as a tunable stiffness element of ATVA [13]. To this end, two leaf springs are used to construct a tunable stiffness element, which can be adjusted by controlling the opening of two leaf springs [15]. Bonello et al. [17] proposed an ATVA with piezo-actuated curved beam, the stiffness of which is varied by adjusting the curvature of each beam. Such an ATVA has many advantages because of their small redundant mass and rapid excited frequency tracking. However, this kind of ATVA is still plagued by many problems that need to be solved, such as reducing damping, improving performance, increasing durability, and so on.

Stability and vibration damping effect are essential in the design of a high-performance ATVA. In practice, the damping of the ATVA should be controlled to a small value to achieve high vibration attenuation performance [22, 23]. However, most materials used in ATVAs have stable damping, which is

*Corresponding author. Tel.: +86 551 3600419, Fax.: +86 551 3600419
E-mail address: gongxl@ustc.edu.cn
† Recommended by Associate Editor Ohseop Song

difficult to decrease. Recently, Xu [24] used a voice coil motor to provide an active force to counteract the damping force. This system improved the vibration attenuation capability of the ATVA considerably. However, active forces that must be introduced to this device increase the complexity and energy consumption of the ATVA. Therefore, some other methods should be considered to further improve vibration reduction. The spring element is the key component of the ATVA when the vibration absorber is working in a vibrating system. The spring elements are usually subjected to a long period of cyclic deformation, often resulting in fatigue failure. This is the soft costal region of ATVA, which requires further investigation.

The vibration attenuation performance should be evaluated as soon as the ATVA prototype is made. Currently, most of the evaluations are implemented on small mass-like platforms with one degree of freedom [11, 16, 20, 25-27]. However, in practice, many primary systems wherein the ATVAs are applied are usually massive multi-mode systems, such as the motors on resilient supporting elements. Some studies have been carried out to attenuate the vibrations of multi-mode systems using vibration absorbers. Brennan and Dayou [28, 29] used a vibration neutralizer to attenuate the global vibration of a multi-mode system (beam). Both theoretical and experimental results proved that the vibration neutralizer can be as effective as an active device at a single frequency in controlling the kinetic energy of the system. Multiple-tuned mass dampers are used to control the vibrations of multi-mode systems that are subjected to broadband excitation, such as certain buildings and machines [30, 31]. The vibration of multi-mode systems can also be controlled by some distinctive vibration absorbers [32, 33]. However, to our knowledge, few studies have focused on the evaluation experiments of the vibration attenuation effect of the ATVA in massive multi-mode systems.

In this paper, a high performance pendulum-like ATVA is designed by introducing a leveraged structure. To improve the efficiency of the ATVA, a spring element with large stiffness can be used to reduce the spring deformation. The pendulum-like ATVA is supposed to be an effective device that can enhance the vibration absorption capacity and further increase resistance to fatigue damage. Finally, a multi-mode experimental platform is designed to investigate the practical vibration adsorption performance of the pendulum-like ATVA. This paper is divided into six sections. Following the introduction, the principle of the pendulum-like ATVA and the comparison between the pendulum-like ATVA and the translational ATVA are analyzed in Section 2. Section 3 describes the pendulum-like ATVA prototype and its dynamic property testing. Section 4 presents the simulations and experiments for the vibration attenuation effect of the pendulum-like ATVA on the multi-mode system. The conclusions are summarized in the final section.

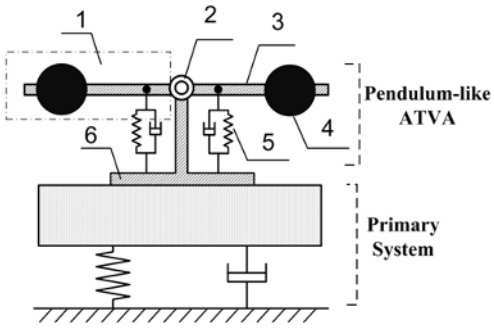

(a)

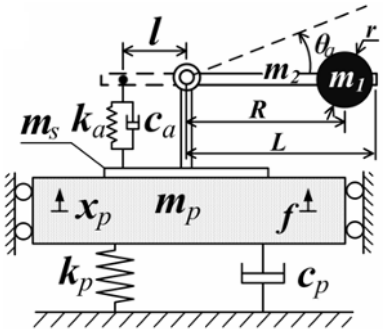

(b)

1. Left dynamic mass; 2. Pendulum axis; 3. Pendulum arm; 4. Cylindrical slider; 5. Spring element; 6. Absorber base.

Fig. 1. Scheme of the primary system with pendulum-like ATVA.

2. Analysis on pendulum-like ATVA

2.1 Working principle

To illustrate the working principle, an SODF primary system with the proposed pendulum-like ATVA is described in Fig. 1(a). The pendulum-like ATVA can be considered as two axisymmetric dynamic masses swaying around the same pendulum axis. It consists of three parts: the static mass, dynamic mass, and the spring-damping system. The static mass is composed of an absorber base and a pendulum axis. The dynamic mass is composed of a pendulum arm and a sliding block. The mass distribution of dynamic mass can be changed by adjusting the position of the sliding blocks at the pendulum axis. Thus, the natural frequency of the pendulum-like ATVA can be controlled by tuning the position of the sliders to trace the external excitation frequency. When the tuned pendulum-like ATVA matches the excitation frequency, the vibration can be attenuated significantly. This point will be theoretically addressed in the following sections.

Given the symmetrical structure of the pendulum-like ATVA, its scheme can be simplified in Fig. 1(b). m_p, k_p, and c_p are the mass, stiffness, and the damping of the primary system, respectively. m_a is the dynamic mass of the pendulum-like ATVA; it is composed of the slider's mass m_1 and the mass of the pendulum arms' mass m_2. m_s is the static mass of the pendulum-like ATVA. k_a and c_a are the

stiffness and damping of the spring element, respectively. l is the distance between the smart spring element and the axis. R is the distance between the centroid of the slider and the axis, and R it can be adjusted to track frequency-varying disturbances. L is the length of the pendulum arm. r is the radius of the cylindrical slider. f is the exciting force applied on the primary system. x_p is the displacement of the primary system. θ_a is the angular displacement of the pendulum-like ATVA. According to Newton's law [34], the equations of motion can be expressed as follows:

$$\begin{cases} [m_1 r^2 + m_1 R^2 + \frac{1}{3} m_2 L^2]\ddot{\theta} + [m_1 R + \frac{1}{2} m_2 L]\ddot{x}_p \\ + c_a l^2 \dot{\theta} + k_a l^2 \theta = 0 \\ [m_p + m_a + (m_1 + m_2)]\ddot{x}_p + (m_1 R + \frac{1}{2} m_2 L)\ddot{\theta} \\ + c_p \dot{x}_p + k_p x_p = f \end{cases} . \tag{1}$$

Defining $\omega_p = \sqrt{k_p / m_p}$, $\xi_p = c_p / (2 m_p \omega_p)$, $\omega_a = \sqrt{k_a / m_a}$, and $\xi_a = c_a / (2 m_a \omega_a)$, where ω_p and ξ_p are the natural frequency and the damping ratio of the primary system, respectively, and ω_a and ξ_a are the relative natural frequency and the damping ratio of the pendulum-like ATVA, respectively. It should be noted Note that ω_a is not equal to the natural frequency of the pendulum-like ATVA. In fact, it is the natural frequency of the translational ATVA whose spring element is the same as that of the pendulum-like ATVA. In this paper, ω_a it is defined as the relative natural frequency. From Eq. (1), the driving point mobility of the primary system with a pendulum-like ATVA attached can be obtained as follows:

$$H_1(\omega) = \frac{X_p(\omega)}{F(\omega)} = \frac{1}{m_p \omega_p^2 [-(1+\mu)\Omega_p^2 - \frac{\mu}{1+\mu_1}(\eta + \frac{\varphi \tilde{L}}{2\tilde{R}})\rho \Omega_p^2 + 2 j \xi_p \Omega_p + 1]} \tag{2}$$

where

$$\rho = \frac{(\eta \tilde{R}^2 + \frac{1}{2}\varphi \tilde{L} \tilde{R})\Omega_a^2}{-(\eta \tilde{r}^2 + \eta \tilde{R}^2 + \frac{1}{3}\varphi \tilde{L}^2)\Omega_a^2 + 2 j \xi_a \Omega_a + 1} . \tag{3}$$

In Eqs. (2) and (3), the non-dimensional parameters are defined as follows:

$$\begin{cases} \mu_1 = \frac{m_s}{m_a},\ \mu = \frac{m_a + m_s}{m_p},\ \eta = \frac{m_1}{m_a},\ \varphi = \frac{m_2}{m_a} \\ \tilde{r} = \frac{r}{l},\ \tilde{L} = \frac{L}{l},\ \tilde{R} = \frac{R}{l},\ \Omega_p = \frac{\omega}{\omega_p},\ \Omega_a = \frac{\omega}{\omega_a} \end{cases} . \tag{4}$$

When the pendulum-like ATVA is removed, the driving point mobility of the primary system can be written as follows:

$$H_0(\omega) = \frac{1}{m_p \omega_p^2 [-\Omega_p^2 + 2 j \xi_p \Omega_p + 1]} . \tag{5}$$

Here, the vibration attenuation effect is defined as the ratio of the driving point mobility of the primary system with and without the pendulum-like ATVA attached. Based on the work of Deng [20] and Xu [24], ratio γ, which reflects the effect of vibration absorption capacity, can be defined as

$$\gamma = 20 \lg |\frac{H_1}{H_0}| = 20 \lg |\frac{-\Omega_p^2 + 2 j \xi_p \Omega_p + 1}{-(1+\mu)\Omega_p^2 - \frac{\mu}{1+\mu_1}(\eta + \frac{\varphi \tilde{L}}{2\tilde{R}})\rho \Omega_p^2 + 2 j \xi_p \Omega_p + 1}| . \tag{6}$$

When the pendulum-like ATVA is working, the natural frequency will be turned to trace the external excitation frequency in real time. Hence,

$$\omega_n = \omega \tag{7}$$

where ω_n is the natural frequency of the pendulum-like ATVA, which can be obtained by setting x_p to zero in Eq. (1).

$$\omega_n = \sqrt{\frac{\omega_a^2}{\eta \tilde{r}^2 + \eta \tilde{R}^2 + \frac{1}{3}\varphi \tilde{L}^2}} \tag{8}$$

Substituting Eq. (8) into Eq. (7), the control strategy of the pendulum-like ATVA can be rewritten as follows:

$$\tilde{R} = \sqrt{\frac{1}{\eta \Omega_a^2} - \tilde{r}^2 - \frac{\varphi \tilde{L}^2}{3\eta}} . \tag{9}$$

If the pendulum-like ATVA is not controlled and the position of the sliders is fixed (the natural frequency of the pendulum-like ATVA is kept at a fixed value), it can be regarded as a pendulum-like TVA. Usually, the natural frequency of the ATVA is fixed at the natural frequency of the primary system.

$$\omega_n = \omega_p \tag{10}$$

Similarly, substituting Eq. (10) into Eq. (7), the position of the sliders can be calculated by

$$\tilde{R} = \sqrt{\frac{\Omega_{ap}^2}{\eta} - \tilde{r}^2 - \frac{\varphi \tilde{L}^2}{3\eta}} \tag{11}$$

where $\Omega_{ap} = \omega_a / \omega_p$.

Generally, various parameters of the primary system are es-

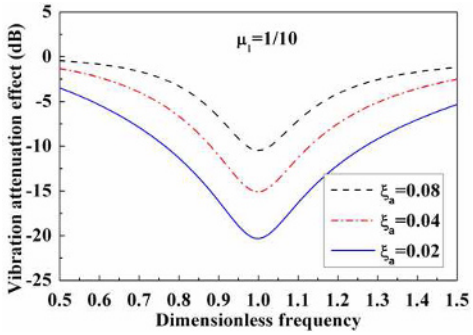

(a) Influence of damping ratio ξ_a

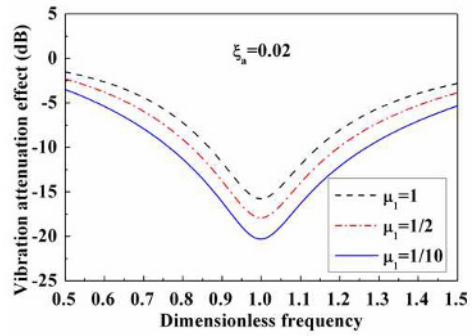

(b) Influence of mass ratio μ_1

Fig. 2. Vibration attenuation effect with different parameters of the pendulum-like ATVA.

tablished established, and the total mass and size of the vibration absorbers have specific restrictions. Therefore, when the mass ratio of the total mass to the primary system μ and the damping ratio of the primary system ξ_p of the vibration absorbers are established, the capacity of the vibration suppression is only related to the damping ratio ξ_a and to the mass ratio of the pendulum-like ATVA. The effect of the vibration absorption capacity can be calculated according to the following parameters: $\mu = 0.02$, $\eta = 0.8$, $\varphi = 0.2$, $\tilde{r} = 1$, $\tilde{L} = 7$ and $\Omega_{ap} = 3.5$. Comparisons of various parameters are shown in Fig. 2.

During the simulation, the dimensionless frequency Ω_p varies from 0.5 to 1.5. Fig. 2(a) is the vibration attenuation effect of the pendulum-like ATVA when the mass ratio μ_1 is fixed at 1/10 and the damping ratios ξ_a are 0.02, 0.04, and 0.08, respectively. Fig. 2(b) is the vibration reduction effect of the pendulum-like ATVA when the damping ratios ξ_a are fixed at 0.02, and the mass ratios are 1, 1/2, and 1/8, respectively. Decreasing the damping and mass ratios is found to cause an increase in the vibration suppression effect. The simulation results further indicate that a smaller damper material, such as a metal material, should be applied during the design of a vibration absorber and that the damping caused by friction between parts should be minimized. To decrease the mass ratio of the vibration absorber μ_1, the mass of the vibration absorber should be located on the moving mass of the vibration absorber.

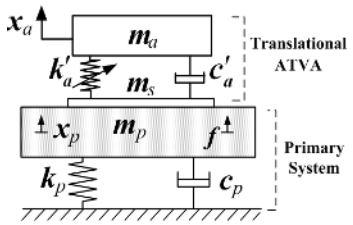

Fig. 3. Scheme of the primary system with translational ATVA.

2.2 Comparison with translational ATVA

2.2.1 Comparison of vibration reduction performance

Compared with the translational ATVA, the pendulum-like ATVA possesses many advantages, although both have the same mass and variation frequency range. According to the Ref. [23], most translational ATVAs can be described as the model shown in Fig. 3.

The translational ATVA is also attached to the SDOF primary system as shown in Fig. 3. m_a and m_s are the dynamic mass and the static mass of the translational ATVA, respectively. They are equal to the values of the pendulum-like ATVA. k'_a is the stiffness of the spring element. It can be adjusted to track frequency-varying disturbances and can be expressed as $k'_a = m_a\omega^2$. Otherwise, if $k'_a = m_a\omega_p^{\ 2}$, the absorber is a translational ATV. c'_a is the damping value of the translational ATVA, and $c'_a = 2m_a\xi_a\omega$, which ensures that the damping of the translational ATVA is equal to that of the pendulum-like ATVA.

According to the dynamic analysis of the above system, the driving point mobility of the primary system with a translational ATVA attached can be obtained as follows [5, 23, 24]:

$$H_2(\omega) = \frac{X_p(\omega)}{F(\omega)} = \frac{1}{m_p\omega_p^2[-(1+\mu)\Omega_p^2 - \frac{\mu}{1+\mu_1}\rho'\Omega_p^2 + 2j\xi_p\Omega_p + 1]} \tag{12}$$

where

$$\rho' = \frac{\Omega_a'^2}{-\Omega_a'^2 + 2j\xi_a\Omega'_a + 1}. \tag{13}$$

In Eq. (13), if Ω'_a is equal to 1, the absorber becomes a translational ATVA, and the natural frequency of the translational ATVA is kept at a fixed value $\Omega'_a = \Omega_p$. In this case, the absorber can be regarded as a translational ATV. The vibration attenuation effect of the translational ATVA can be obtained according to Eqs. (5) and (12) as follows:

$$\gamma' = 20\lg|\frac{H_2}{H_0}| = 20\lg|\frac{-\Omega_p^2 + 2j\xi_p\Omega_p + 1}{-(1+\mu)\Omega_p^2 - \frac{\mu}{1+\mu_1}\rho'\Omega_p^2 + 2j\xi_p\Omega_p + 1}|. \tag{14}$$

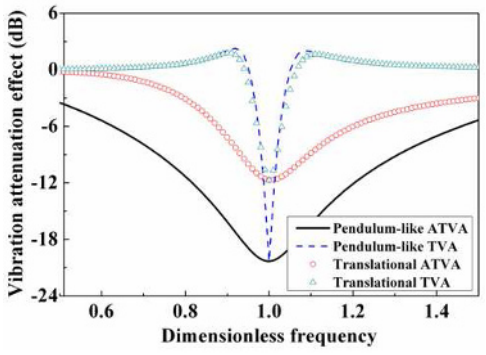

Fig. 4. Vibration attenuation performances of different vibration absorbers.

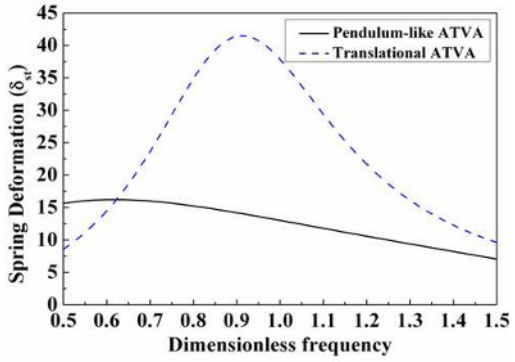

Fig. 5. Comparison of the spring deformation.

The comparison of four kinds of vibration absorbers with the same mass and damping ratios is shown in Fig. 4. Both the pendulum-like ATVA and the translational ATVA have better performance than the TVA. For TVAs, the best vibration attenuation effect occurs at its natural frequency. When the excitation frequency is far from this frequency, the effect decreases quickly. For the entire frequency range, the curve of the attenuation effect of the pendulum-like ATVA is above that of the translational ATVA, which indicates that the pendulum-like ATVA attenuation has a much better performance than the translational ATVA. Moreover, the pendulum-like TVA also has better attenuation effect than the translational TVA at its natural frequency.

The above phenomenon corresponds to the presence of the leveraged structure because it can reduce the damping of the pendulum-like ATVA. To simplify the illustration, the mass of the pendulum arms and the dimensions of the radius of the cylindrical slider are neglected. Then, the first expression in Eq. (1) can be written as

$$m_1\ddot{y}_a + \tilde{R}^2 c_a \dot{y}_a + \tilde{R}^2 k_a y_a = -m_1\ddot{x}_p, \quad y_a = R\theta . \tag{15}$$

Compared with the translational ATVA, Eq. (15) shows that the damping of the pendulum-like ATVA is proportional to $\tilde{R}^2$. In addition, $\tilde{R}^2 < 1$, which means that the damping of the pendulum-like ATVA is smaller than that of the translational ATVA. Therefore, the vibration absorption capacity of the pendulum-like ATVA is much larger than that of the translational ATVA.

2.2.2 Comparison of the spring element deformation

Another advantage of the pendulum-like ATVA is the strength of its spring. The spring, which is one of the most important components of the ATVA, can easily cause fatigue failure when the vibration absorber is working in the vibrating system because of long periods of cyclic deformation. In low-frequency vibration control in particular, the stiffness of the spring elements is often smaller than that in high-frequency vibration control. Therefore, spring elements have larger deformation and can easily result in fatigue damage. However, this issue can be properly solved by the pendulum-like ATVA. Given the institution of pendulum arms in the vibration absorbers, the spring stiffness of the spring element has a much larger value and a smaller deformation than that in the translational ATVA at the same natural frequency.

The larger deformation of the spring element can be calculated easily in an oscillation cycle at a fixed frequency according to the displacement of the primary system. The deformation of the spring element in the pendulum-like ATVA is

$$l_k = \tilde{r}\rho X_p(\omega) = \frac{\rho \cdot \delta_{st}}{\tilde{R}[-(1+\mu)\Omega_p^2 - \frac{\mu}{1+\mu_1}(\eta + \frac{\varphi\tilde{L}}{2\tilde{R}})\rho\Omega_p^2 + 2j\xi_p\Omega_p + 1]} \tag{16}$$

where $\delta_{st} = P_0/k_p$, which is the deformation of the primary system under static load P_0.

For the translational ATVA, the deformation of the spring element is

$$l_k' = \frac{\rho'}{-(1+\mu)\Omega_p^2 - \frac{\mu}{1+\mu_1}\rho'\Omega_p^2 + 2j\xi_p\Omega_p + 1} \cdot \delta_{st} . \tag{17}$$

Comparisons of the spring element deformation between the pendulum-like ATVA and the translational ATVA are shown in Fig. 5.

The deformation of the spring element is found to decrease slightly with the increase of the excitation frequency. The curve is also found to change gently. However, the spring element deformation of the translational ATVA gradually increases when the excitation frequency approaches the natural frequency of the primary system. At most ranges of frequency, the simulation results show that the spring element deformation in the translational ATVA is much larger than that in the pendulum-like ATVA. Hence, the small and stable spring element deformation effectively improves the ability of the ATVA to resist fatigue damage and to extend the service life of vibration absorbers.

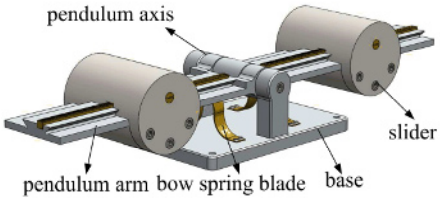

(a) Pendulum-like ATVA

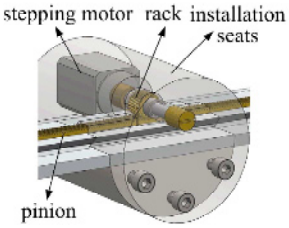

(b) Slide

Fig. 6. Scheme of pendulum-like ATVA.

3. The design and dynamic property of the pendulum-like ATVA

3.1 The prototype of the pendulum-like ATVA

According to the previous analysis, the pendulum-like ATVA performs better than the translational ATVA in terms of vibration reduction and fatigue damage resistance. These results indicate that the pendulum-like ATVA is more suitable for engineering applications. In this paper, a mechanical pendulum-like ATVA is designed and can be considered as two axisymmetric dynamic masses swaying around the same pendulum axis. The model of the pendulum-like ATVA is shown in Fig. 6.

As shown in Fig. 6, the pendulum-like ATVA is composed of pendulum arms, pendulum axis, base, cylindrical sliders, and a bow spring blade. The cylindrical slider consists of a stepping motor and its installation seats. The cylindrical slider and the pendulum arms are jointed with the rack and pinion to ensure accuracy in transmission. By using a stepping motor, the slider can move freely along the pendulum arm, and the natural frequency of the pendulum-like ATVA can be changed to trace the external excitation frequency. The stepping motor must function as a self-locking stepping motor to ensure that the pendulum-like ATVA works as a TVA when the control system fails. The cylindrical sliders and the pendulum arms constitute the dynamic mass of the pendulum-like ATVA. The stepping motor, which acts as a part of the dynamic mass, can make best use of the space and raise the utilization of mass. The bow spring blade should be chosen for its good holding capacity and large lateral rigidity. It should also meet the requirements of long-term cycle deformation use with stability and low cost.

3.2 Dynamic characteristics of the prototype

A vibration table is used to study the dynamic properties of the pendulum-like ATVA. The schematic of the testing system is shown in Fig. 7.

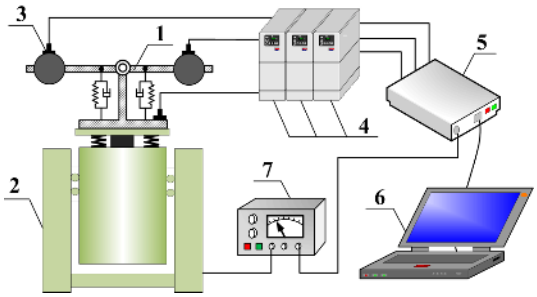

1. Pendulum-like ATVA; 2.Vibration table; 3. Accelerometer
4. Charge amplifiers; 5. Dynamic signal analyzer; 6. Computer.

Fig. 7. Schematic of the test system for the measurement of the dynamic properties of the prototype.

The pendulum-like ATVA is fixed on a vibration table. The signal analyzer provides a sweep sinusoidal excitation signal to drive the system via a power amplifier. Two accelerometers (model: CA-YD, manufactured by Sinocera Piezotronics Inc., China) are placed on the pendulum arm, and one accelerometer is placed on the vibration table to record their responses. The acceleration signals of the vibration table and the pendulum arm are then sent to the dynamic signal analyzer (SignalCalc430, Data Physics Corporation, USA) with the input signals and the output signal of the prototype. With these signals, the transmissibility relating the output signal to the input signal can be obtained using fast Fourier transform (FFT) analysis in the dynamic signal analyzer. The peak of the transmissibility curve is the natural frequency of the prototype. With the transmissibility curve, the damping ratio can be computed using the half power bandwidth method.

Fig. 8 shows the amplitude-frequency curves and the phase-frequency curves of the transmissibility of the left pendulum arm. The results indicate that transmissibility curves move rightward by reducing the distance R between the centroid of the slider and the axis, which means that the natural frequency of the pendulum-like ATVA varies with distance R.

By reading the peak values of the transmissibility in Fig. 8, the obtained frequency-shift property of the left pendulum arm is shown in Fig. 9(a).

As described in this figure, the natural frequency of the left pendulum arm changes from 10.25 Hz to 21.25 Hz when the distance R varies from 17 cm to 6 cm. Therefore, the pendulum-like ATVA prototype has the capability to change its frequency by 207%. Using the same method, the frequency-shift property of the right pendulum arm can also be obtained. The natural frequency of the right pendulum arm varies from 10.25 Hz to 21 Hz, which is much closer to the right pendulum arm. Moreover, the experiment values are well agreed with the theoretical values. The damping ratios obtained by using the half power bandwidth method are shown in Fig. 9(b). The average damping ratio is roughly 0.022, indicating that tthe which demonstrates that the damping of the pendulum-like prototype is low.

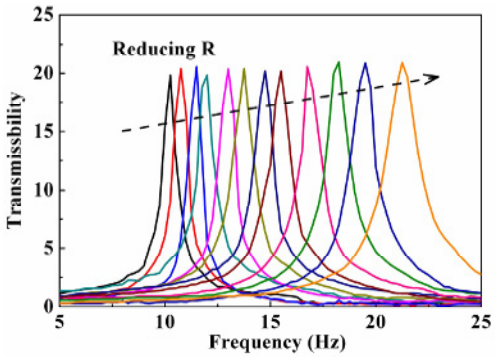

(a) Amplitude-frequency curve

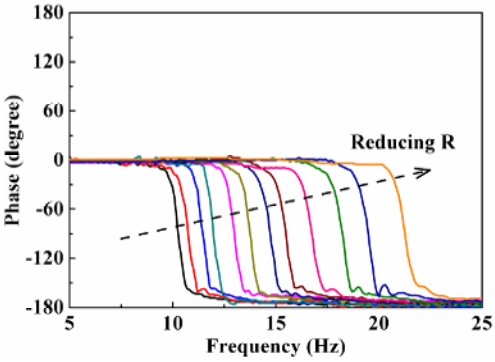

(b) Phase-frequency curve

Fig. 8. Transmissibility versus frequency at various distances *R*.

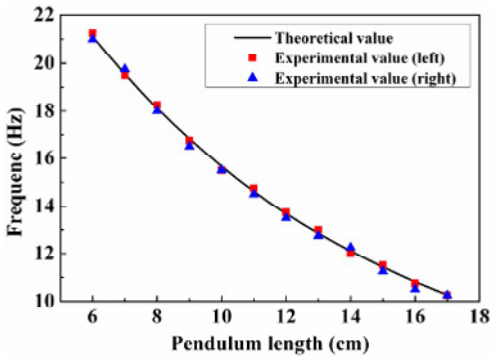

(a) Frequency-shift property

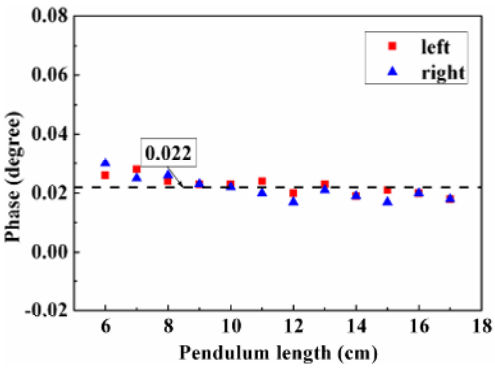

(b) Damping property

Fig. 9. Testing results of the dynamic properties.

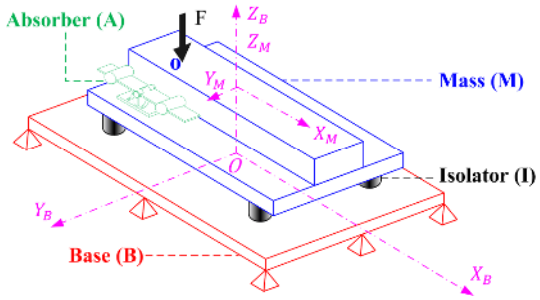

Fig. 10. Simulation model of the multi-mode system with the pendulum-like ATVA attached.

4. Vibration attenuation effect evaluation on a multi-model platform

4.1 Numerical simulation of the vibration attenuation effect

Many systems suffering from undesired vibrations are essentially multi-mode systems. Some simulations are carried out to evaluate the vibration attenuation performance of the pendulum-like ATVA used in such systems. The simulation model shown in Fig. 10 comprises a machine as the mass, a rectangular plate with four supporting edges as the flexible base, and four isolators between the mass and the base. In engineering applications, the vertical vibration energy is more significant than that of other directions especially in a low-frequency band. Thus, only the vertical forces and the resulting motions of the system are given focus in this model. By assembling the mobility matrices of the subsystems [35, 36], the mathematical models of the system can be implemented.

4.1.1 Mathematical model of the simulation

Neglecting elasticity, the mass is treated as a rigid body with three modes. Assuming $P_l(x_l, y_l)$ and $P_s(x_s, y_s)$ are the coordinates of any two points on the mass, according to literature [34, 36], the acceleration cross mobility between them according to literature [34, 36] is:

$$\xi(P_l, P_s) = \frac{1}{m_M} + \frac{x_l x_s}{J_x} + \frac{y_l y_s}{J_y} \tag{18}$$

where m_M is the mass of the mass, J_x is the rotational inertia of the mass of the X axis, and J_y is the rotational inertia of the mass of the Y axis. The equation describing the mass is

$$\begin{bmatrix} Acc_{Mt} \\ \mathbf{Acc}_{Mb} \end{bmatrix} = \mathbf{M}_M \begin{bmatrix} F_{Mt} \\ \mathbf{F}_{Mb} \end{bmatrix} = \begin{bmatrix} M_{11} & \mathbf{M}_{12} \\ \mathbf{M}_{21} & \mathbf{M}_{22} \end{bmatrix} \begin{bmatrix} F_{Mt} \\ \mathbf{F}_{Mb} \end{bmatrix} \tag{19}$$

where $\mathbf{M}_M$ is the mobility matrix of the mass, and $\mathbf{Acc}$ and $\mathbf{F}$ are the acceleration and force vectors, respectively. The subscripts M, b and t denote substructure mass, top, and bottom interfaces, respectively. Similarly, the acceleration and force vectors of the isolators and base are defined as $\mathbf{Acc}_{It}$, $\mathbf{Acc}_{Ib}$, $\mathbf{F}_{It}$ and $\mathbf{F}_{Ib}$; $\mathbf{Acc}_B$ and $\mathbf{F}_B$.

The sub-matrices of $\mathbf{M}_M$ are

$$M_{11}=[\xi(P_F,P_F)] \quad \mathbf{M}_{12}=[\xi(P_F,P_l)]_{1\times4}$$
$$\mathbf{M}_{21}=\mathbf{M}_{12}^T \quad \mathbf{M}_{22}=[\xi(P_l,P_s)]_{4\times4} \quad (l,s=1,2,3,4)$$

with P_F and P_l representing the position coordinates of the exciting force and the four isolators.

The mass attached to the pendulum-like ATVA will affect its mobility matrix. Setting x_p, k_p and c_p to zero in Eq. (1), we can obtain the acceleration admittance at the setting point of the pendulum-like ATVA.

$$M_A=\frac{Acc_A}{F_A}=\frac{1}{m_a[1+(\eta+\frac{\varphi\tilde{L}}{2\tilde{R}})\rho]} \tag{20}$$

The Acc_A and F_A are the acceleration and force vectors at the setting point of the pendulum-like ATVA, respectively. In considering the force applied on the pendulum-like ATVA, the equation describing the mass with the pendulum-like ATVA attached is altered as:

$$\begin{bmatrix} Acc_{Mt} \\ \mathbf{Acc}_{Mb} \\ Acc_A \end{bmatrix}=\begin{bmatrix} \mathbf{M}_M & \mathbf{M}_{AM} \\ \mathbf{M}_{Ma} & M_{AA} \end{bmatrix}\begin{bmatrix} F_{Mt} \\ \mathbf{F}_{Mb} \\ F_A \end{bmatrix} \tag{21}$$

where

$$\mathbf{M}_{Am}=[\xi(P_a,P_F)\ \ \xi(P_a,P_1)\ \ \xi(P_a,P_2)\ \ \xi(P_a,P_3)\ \ \xi(P_a,P_4)]^T,$$
$$\mathbf{M}_{mA}=\mathbf{M}_{AM}{}^T,$$
$$M_{AA}=[\xi(P_a,P_a)] \quad (a=A,B,C).$$

With P_a representing the position coordinate with the setting point of the pendulum-like ATVA, the pendulum-like ATVA can be mounted in there are three locations (A, B, C) to choose from to mount on the pendulum-like ATVA. By combining Eqs. (20) and (21), Acc_A and F_A can be eliminated from Eq. (21). The modified equation is:

$$\begin{bmatrix} Acc_{Mt} \\ \mathbf{Acc}_{Mb} \end{bmatrix}=\hat{\mathbf{M}}_M\begin{bmatrix} F_{Mt} \\ \mathbf{F}_{Mb} \end{bmatrix}$$
$$=[\mathbf{M}_M+\mathbf{M}_{Am}(M_A-M_{AA})\mathbf{M}_{mA}]\begin{bmatrix} F_{Mt} \\ \mathbf{F}_{Mb} \end{bmatrix}. \tag{22}$$

According to Ref. [34], the model of the isolator is a spring-mass system (Fig. 11). To introduce the mass of the isolator into the simulation, a lumped mass m_I is placed at the middle of the spring. The complex stiffness $k_I^*=k_I(1+jg)$ is used to describe the stiffness characteristic of the isolator, which is made of a rubber material. g is the loss factor of the material. The lumped mass divides the spring into two minor springs with complex stiffness $2k_I^*$.

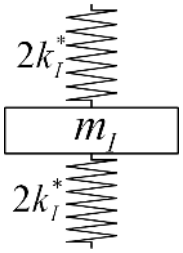

Fig. 11. Model of the isolator.

The equation describing the substructure isolators is

$$\begin{bmatrix} \mathbf{Acc}_{It} \\ \mathbf{Acc}_{Ib} \end{bmatrix}=\mathbf{M}_I\begin{bmatrix} \mathbf{F}_{It} \\ \mathbf{F}_{Ib} \end{bmatrix}=\begin{bmatrix} \mathbf{I}_{11} & \mathbf{I}_{12} \\ \mathbf{I}_{21} & \mathbf{I}_{22} \end{bmatrix}\begin{bmatrix} \mathbf{F}_{It} \\ \mathbf{F}_{Ib} \end{bmatrix} \tag{23}$$

where

$$\mathbf{I}_{11}=\mathbf{I}_{22}=diag[\frac{-\omega^2}{2k_I^*}+\frac{1}{m_I}]_{4\times4},$$
$$\mathbf{I}_{12}=\mathbf{I}_{21}=diag[\frac{1}{m_I}]_{4\times4}.$$

According to the vibration theory of the flexible board [34-36], the cross of the flexible base mobility between any two points on the plane P_u, P_v is written as

$$\chi(P_u,P_v)=-\frac{\omega^2}{m_B}\sum_{m=1}^{N}\sum_{n=1}^{N}\frac{\phi_{mn}(P_u)\phi_{mn}(P_v)}{\omega_{mn}^2(1+j\delta)-\omega^2} \tag{24}$$

where m_B is the mass of the plane, δ is the loss factor of the plane, and ω_{mn} and ϕ_{mn} are the natural angular frequency and the mode function of the plane, respectively. N is the number of the mode that is taken into account. The equation describing the substructure base is

$$\mathbf{Acc}_B=\mathbf{M}_B\mathbf{F}_B=[\chi(P_u,P_v)]_{4\times4}\mathbf{F}_B \quad (u,v=1,2,3,4). \tag{25}$$

By assembling all the obtained mobility matrices of the subsystems ($\mathbf{M}_M$, $\mathbf{M}_I$ and $\mathbf{M}_B$), the mathematical models of the entire system can be established. The relationship between the transmitted forces and the corresponding accelerations on the interfaces of the subsystems can be easily determined as

$$\begin{matrix} \mathbf{F}_{Mb}=-\mathbf{F}_{It} & \mathbf{Acc}_{Mb}=\mathbf{Acc}_{It} \\ \mathbf{F}_{Ib}=-\mathbf{F}_B & \mathbf{Acc}_{Ib}=\mathbf{Acc}_B \end{matrix}. \tag{26}$$

By combining Eqs. (19), (23), (25) and (26), the acceleration of the excitation point can be obtained as

$$\mathbf{Acc}_B=\mathbf{M}_B\mathbf{H}_B\mathbf{H}_AF_{Mt} \tag{27}$$

where

$$\mathbf{H}_A = (\mathbf{M}_{22} + \mathbf{I}_{11} - \mathbf{I}_{12}\mathbf{H}_B)^{-1}\mathbf{M}_{21}$$
$$\mathbf{H}_B = (\mathbf{M}_B + \mathbf{I}_{22})^{-1}\mathbf{I}_{21}$$

With Eqs. (22) and (27), the response of the system with the pendulum-like ATVA attached can be computed by replacing the sub-matrices of $\mathbf{M}_M$ with that of $\hat{\mathbf{M}}_M$. When the pendulum-like ATVA is attached to the multi-mode system, the dynamic characteristics of the system will be changed. In this workstudy, the attenuation of the average vibration of the flexible base is used to represent the vibration attenuation effect of the pendulum-like ATVA. The vibration attenuation effect of the pendulum-like ATVA is stated as follows:

$$\gamma = 20\lg\left|\frac{\overline{Acc_{b-with}}}{\overline{Acc_{b-without}}}\right| \tag{28}$$

where $\overline{Acc_{b-with}}$ and $\overline{Acc_{b-without}}$ are the average acceleration responses of the flexible base with and without the DVA attached, respectively. They can be calculated by the following formula as

$$\overline{Acc_b} = \sqrt{\frac{\sum_{i=1}^{4} Acc_{Bi}}{4}} \tag{29}$$

where Acc_{Bi} is the vibration acceleration amplitude of the number i test point on the flexible base. The smaller the γ is, the better the effect that can be achieved.

4.1.2 Simulation results

In the simulation, the concerned frequency band ranged from 10 Hz to 20 Hz. Corresponding to subsequent experiments, the following data are used in the calculations:

$$F_{Mt} = e^{j\omega t} \qquad P_F = (-0.35, 0)$$
$$m_M = 300Kg \qquad J_Y = 25Kg\cdot m^2 \qquad J_X = 5.2Kg\cdot m^2$$
$$m_1 = 0.5Kg \qquad g = 0.14 \qquad k_1 = 744193N/m$$
$$m_B = 1092Kg \qquad \delta = 0.05 \qquad P_1 = (\pm 0.22, \pm 0.3)$$
$$m_a = 4.5Kg \qquad \tilde{r} = 1 \qquad k_a = 612500N/m$$
$$\xi_a = 0.022 \qquad \tilde{L} = 7 \qquad (\varphi = 0.8, \eta = 0.2)$$
$$P_A = (-0.35, 0.25) \qquad P_B = (-0.35, 0) \qquad P_C = (-0.35, -0.25)$$

If only the vertical vibration is considered, the system will have three vibration modes: vertical vibration mode, rotation mode around the X-axis, and rotation mode around the Y-axis. The undamped natural frequencies of three modes can be determined as follows:

$$f_{vertical} = \frac{1}{2\pi}\sqrt{\frac{4k_1}{m_m}} = \frac{1}{2\pi}\sqrt{\frac{4\times 744193}{300}} \approx 16Hz,$$

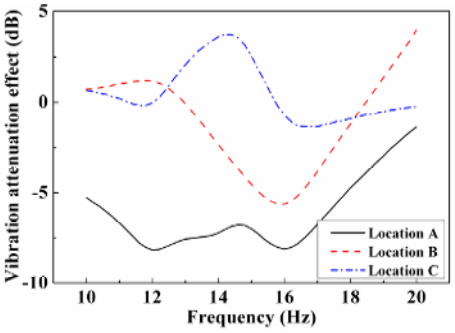

Fig. 12. Simulation results of the vibration attenuation effect.

$$f_{X-axis} = \frac{1}{2\pi}\sqrt{\frac{4k_1C_{i-y}^2}{J_x}} = \frac{1}{2\pi}\sqrt{\frac{4\times 744193\times 0.2^2}{5.2}} \approx 24Hz,$$
$$f_{Y-axis} = \frac{1}{2\pi}\sqrt{\frac{4k_1C_{i-x}^2}{J_y}} = \frac{1}{2\pi}\sqrt{\frac{4\times 744193\times 0.22^2}{25}} \approx 12Hz.$$

The excitation force is applied along the X-axis, which is the nodal line of the rotation mode around the X-axis; therefore, this mode cannot be excited.

Fig. 12 shows the simulation results. When the excitation frequency is close to 16 Hz, the vertical vibration mode contributes considerably to the vibration. The pendulum-like ATVA fixed at any position can exert positive effects on attenuating the vibration because this mode has no nodal line. Bordered by the Y-axis, the pendulum-like ATVA located on the same side of the excitation is found to work better. The farther the installation location is away from the nodal line, the better the effect that can be obtained.

The vibration with the frequency closest to 12 Hz depends primarily on the rotation mode of the Y-axis. Therefore, the vibration can be attenuated by the pendulum-like ATVA except when a nodal line of this mode (Y-axis) is installed. The situation is similar when the frequency is close to 16 Hz. However, the effect is more obvious when the pendulum-like ATVA is placed on the same side of the excitation.

If the excitation frequency lies between 12 and 16 Hz, the pendulum-like ATVA on the same side of the excitation force will have evident vibration attenuation effect. However, the pendulum-like ATVA on the opposite side receives a negative result, indicating that the vibration of the system is increased by the pendulum-like ATVA. The simulation results indicate that the ATVA should be installed on the same side of the excitation.

4.2 Evaluation experiments of the vibration attenuation effect

To evaluate the vibration attenuation effect of the prototype of the pendulum-like ATVA, a massive multi-mode platform is designed in accordance with the theoretical model in Fig. 10. Fig. 13 shows the photograph of the experimental platform. A rigid mass supported by four rubber isolators is fixed on the

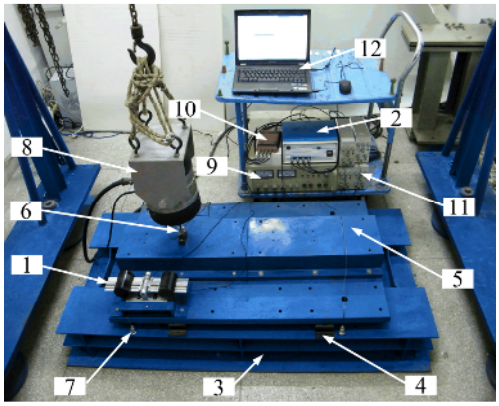

1. Pendulum-like ATVA; 2. Control box; 3. Flexible base;
4. Isolator; 5. Mass; 6. Impedance head; 7. Accelerometer;
8. Excitation; 9. Power amplifier; 10. Dynamic signal analyzer;
11. Charge amplifiers; 12. Computer.

Fig. 13. Photograph of the experimental set-up.

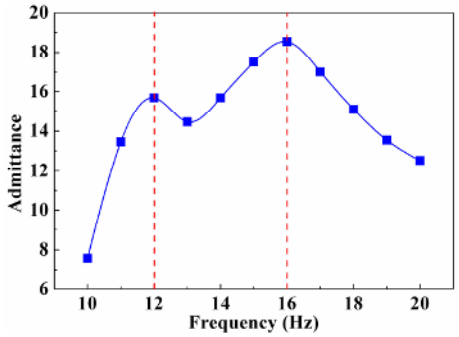

Fig. 14. Admittance of the evaluation platform.

elastic base welded by steel plates. The natural frequencies of the elastic base are much larger than that of the mass. Therefore, the vibration of the system is mainly affected by the modes of the mass in the low frequency. The major parameters of the platform, such as mass, rotation inertia, and stiffness of the isolator are similar to that used in simulation. The pendulum-like ATVA is placed on one side of the mass. The eccentric excitation is applied by an electromagnetic exciter. An impedance head connecting the mass and the exciter is used to monitor the acceleration and force signals. Four accelerometers are placed near the isolators to measure the vibration of the flexible base. As the mass of the platform is 300 kg. the ratio of the mass of the platform and the mass of the pendulum-like ATVA is 60:1.

With these signals measured by the impedance head, the admittance relating the acceleration to the force signal is obtained through FFT analysis. The admittance spectrum of the system without an absorber attached is shown in Fig. 14. Here, two peaks corresponding to the rotation mode and the vertical vibration mode are found in the curve.

In this experiment, the system is excited by a series of single frequencies to approximate a swept sine excitation. The amplitude of the excitation force is 80 N, and the frequency

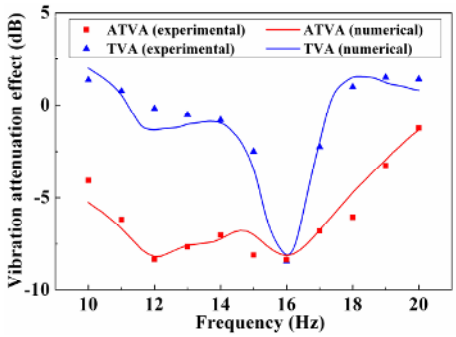

Fig. 15. Experimental results of the vibration attenuation effect.

range is 10 Hz to 20 Hz. The pendulum-like ATVA is controlled by a control box composed of a step motor driver (SH-20403, Beijing Hollysys Inc., China) and a self-made processor with a core of DSP-TMS320F2812 (Texas instrument Company, USA). Before the control process is started, the initial frequency of the pendulum-like ATVA, the relational table between the natural frequency, and the position of the sliding blocks at the pendulum axis are set. When the pendulum-like ATVA is working, the signals of vibration of the experimental platform are sampled by the control system. The sampling time interval and the sampling numbers are 0.001 s and 1024, respectively. Through the sampled signal, we can obtain the dominant frequency of the excitation force by FFT. A look-up table is then used to compute the desired position and to drive the motor further to tune the slider to the desired position at the pendulum axis. In this way, the control system can adjust the frequency of the pendulum-like ATVA to trace the external excitation frequency as rapidly as possible. According to Eq. (28), the vibration attenuation effect is characterized by comparing the average vibration of the flexible base with and without an absorber (TVA and ATVA).

Fig. 15 shows the experimental results of the vibration attenuation effect. The ratio of the platform and the absorber mass is about 60, and the pendulum-like ATVA is fixed on location A (the same side with the excitation), as shown in Fig. 10. If the natural frequency is fixed at 16 Hz, the uncontrolled pendulum-like ATVA can be regarded as a pendulum-like TVA. For the pendulum-like TVA, the best vibration attenuation effect occurs at its natural frequency. The effect goes down when the excitation frequency is far from this frequency. At some frequencies, the values of the effects are even larger than 0, indicating that the vibration of the system is increased by the pendulum-like TVA. For the ATVA whose natural frequency is tuned to trace the excitation frequency, its vibration attenuation effect is better than that of the TVA within the entire adjustable frequency band except at 16 Hz. The curve has two troughs at the natural frequencies of the system (12 and 16 Hz), which means that the pendulum-like ATVA works much better in attenuating large vibrations. The best effect of the pendulum-like ATVA reaches roughly 8.5 dB at 12 Hz. The numerical results of the vibration attenuation effect are computed with the method presented in Section 4. A

comparison between the simulation results and experimental data is conducted. Fig. 15 shows that the experimental data and numerical curve are very close. The average error between the experimental data and the simulation results is smaller than 0.52 dB for the pendulum-like ATVA, and the value of this index is smaller than 0.48 dB for the pendulum-like ATVA. The main error lies in the setting of the boundary conditions and in the usage of simplified theoretical models. The results indicate that the dynamic model is reasonable and that the experimental data are reliable.

5. Conclusions

In this work, a novel pendulum-like ATVA that consists of two axisymmetric pendulum arms swaying around the same pendulum axis is developed. The natural frequency of this ATVA can be tuned from 10.25 Hz to 21 Hz by adjusting the distance R between the centroid of the slider and the pendulum axis, which varies from 17 cm to 6 cm. The damping of the prototype is rather small, and the average damping ratio is 0.022. Compared with translational ATVA, the pendulum-like ATVA decreases the damping of the ATVA as well as the deformation of the spring. Hence, the vibration absorption capacity is enhanced, and resistance to fatigue damage ability is increased.

To investigate the vibration adsorption performance, simulations are carried out using the transmission mobility method to predict the vibration characteristics of the multi-mode system with the pendulum-like ATVA attached theoretically. The pendulum-like ATVA fixed on location A is found to be capable of controlling all the modes of the system and to receive a good effect within a frequency range. The simulation results are verified through experimental studies conducted on a multi-mode platform comprising a mass, isolator, and a flexible base. The experimental results demonstrate that the pendulum-like ATVA mounted on location A can reduce the vibration effectively in a broad frequency range. The best effect reaches 8.5 dB when the ratio of the mass of the platform and the mass of the pendulum-like ATVA is roughly 60:1. The experimental results agree well with the theoretical calculation. Therefore, this kind of pendulum-like ATVA has great potential in engineering applications.

Acknowledgment

Financial support from the National Natural Science Foundation of China (Grant No. 11125210) and the Funds of the Chinese Academy of Sciences for Key Topics in Innovation Engineering (Grant No. KJCX2-EW-L02) are gratefully acknowledged.

References

[1] H. Frahm, Device for damping vibrations of bodies, U.S. Patent: 989958 (1909).

[2] J. T. Chung, Vibration absorber for reduction of the in-plane vibration in an optical disk drive, *Ieee Transactions on Consumer Electronics*, 50 (2) (2004) 552-557.

[3] T. X. Wu, On the railway track dynamics with rail vibration absorber for noise reduction, *Journal of Sound and Vibration*, 309 (3-5) (2008) 739-755.

[4] A. C. Webster and R. Vaicaitis, Application of tuned mass dampers to control vibrations of composite floor systems, *Engineering Journal-American Institute of Steel Construction Inc*, 29 (3) (1992) 116-124.

[5] H. Mori, O. Mikhyeyev, T. Nagamine, M. Mori and Y. Sato, Effect of a dynamic absorber on friction-induced vibration of a rectangular plate, *Journal of Mechanical Science and Technology*, 24 (1) (2010) 93-96.

[6] L. D. Viet and Y. Park, Vibration control of the axisymmetric spherical pendulum by dynamic vibration absorber moving in radial direction, *Journal of Mechanical Science and Technology*, 25 (7) (2011) 1703-1709.

[7] D. J. Inman, *Engineering Vibration*, *Prentice–Hall*, Englewood Cliffs, USA (1994).

[8] M. J. Brennan, Actuators for active vibration control - Tunable resonant devices, *Applied Mechanics and Engineering*, 5 (1) (1999) 63-74.

[9] J. Q. Sun, M. R. Jolly and M. A. Norris, Passive, adaptive and active tuned vibration absorbers - a survey, *Journal of Mechanical Design*, 117 (1995) 234-242.

[10] A. H. von Flotow, Adaptive tuned vibration absorbers: tuning laws, tracking agility, sizing and physical implementation, *Proceedings of Noise-Con*, 94 (1994) 81-101.

[11] N. Jalili and B. Fallahi, Design and dynamic analysis of an adjustable inertia absorber for semiactive structural vibration attenuation, *Journal of Engineering Mechanics-Asce*, 128 (12) (2002) 1342-1348.

[12] M. A. Franchek, M. W. Ryan and R. J. Bernhard, Adaptive passive vibration control, *Journal of Sound and Vibration*, 189 (5) (1996) 565-585.

[13] K. Nagaya, A. Kurusu, S. Ikai and Y. Shitani, Vibration control of a structure by using a tunable absorber and an optimal vibration absorber under auto-tuning control, *Journal of Sound and Vibration*, 228 (4) (1999) 773-792.

[14] J. P. Carneal, F. Charette and C. R. Fuller, Minimization of sound radiation from plates using adaptive tuned vibration absorbers, *Journal of Sound and Vibration*, 270 (4-5) (2004) 781-792.

[15] P. L. Walsh and J. S. Lamancusa, A variable stiffness vibration absorber for minimization of transient vibrations, *Journal of Sound and Vibration*, 158 (2) (1992) 195-211.

[16] M. R. F. Kidner and M. J. Brennan, Varying the stiffness of a beam-like neutralizer under fuzzy logic control, *Journal of Vibration and Acoustics-Transactions of the ASME*, 124 (1) (2002) 90-99.

[17] P. Bonello, M. J. Brennan and S. J. Elliott, Vibration control using an adaptive tuned vibration absorber with a variable curvature stiffness element, *Smart Materials & Structures*, 14 (5) (2005) 1055-1065.

[18] J. Liu and K. F. Liu, A tunable electromagnetic vibration absorber: Characterization and application, *Journal of Sound and Vibration*, 295 (3-5) (2006) 708-724.
[19] E. Rustighi, M. J. Brennan and B. R. Mace, A shape memory alloy adaptive tuned vibration absorber: design and implementation, *Smart Materials & Structures*, 14 (1) (2005) 19-28.
[20] H. X. Deng, X. L. Gong and L. H. Wang, Development of an adaptive tuned vibration absorber with magnetorheological elastomer, *Smart Materials & Structures*, 15 (5) (2006) N111-N116.
[21] X. Z. Zhang and W. H. Li, Adaptive tuned dynamic vibration absorbers working with MR elastomers, *Smart Structures and Systems*, 5 (5) (2009) 517-529.
[22] M. J. Brennan, Vibration control using a tunable vibration neutralizer, Proceedings of the Institution of Mechanical Engineers Part C, *Journal of Mechanical Engineering Science*, 211 (2) (1997) 91-108.
[23] H. L. Sun, P. Q. Zhang, X. L. Gong and H. B. Chen, A novel kind of active resonator absorber and the simulation on its control effort, *Journal of Sound and Vibration*, 300 (1-2) (2007) 117-125.
[24] Z. B. Xu, X. L. Gong, G. J. Liao and X. M. Chen, An active-damping-compensated magnetorheological elastomer adaptive tuned vibration absorber, *Journal of Intelligent Material Systems and Structures*, 21 (10) (2010) 1039-1047.
[25] K. F. Liu, L. Liao and J. Liu, Comparison of two auto-tuning methods for a variable stiffness vibration absorber, *Transactions of the Canadian Society for Mechanical Engineering*, 29 (1) (2005) 81-96.
[26] M. Kidner and M. J. Brennan, Improving the performance of a vibration neutraliser by actively removing damping, *Journal of Sound and Vibration*, 221 (4) (1999) 587-606.
[27] N. Olgac and C. Huang, On the stability of a tuned vibration absorber for time varying multiple frequencies, *Journal of Vibration and Control*, 8 (4) (2002) 451-465.
[28] J. Dayou and M. J. Brennan, Optimum tuning of a vibration neutralizer for global vibration control, *Proceedings of the Institution of Mechanical Engineers Part C-Journal of Mechanical Engineering Science*, 215 (C8) (2001) 933-942.
[29] J. Dayou and M. J. Brennan, Experimental verification of the optimal tuning of a tunable vibration neutralizer for global vibration control, *Applied Acoustics*, 64 (3) (2003) 311-323.
[30] R. S. Jangid and T. K. Datta, Performance of Multiple Tuned Mass dampers for torsionally coupled system, *Earthquake Engineering & Structural Dynamics*, 26 (3) (1997) 307-317.
[31] W. J. Hsueh, Vibration transmissibility of a unidirectional multi degree of freedom system with multiple dynamic absorbers, *Journal of Sound and Vibration*, 229 (4) (2000) 793-805.
[32] L. Zuo and S. A. Nayfeh, Minimax optimization of multi-degree-of-freedom tuned-mass dampers, *Journal of Sound and Vibration*, 272 (3-5) (2004) 893-908.
[33] S. A. Vera, M. Febbo, C. G. Mendez and R. Paz, Vibrations of a plate with an attached two degree of freedom system, *Journal of Sound and Vibration*, 285 (1-2) (2005) 457-466.
[34] S. S. Rao, Mechanical vibrations, fourth edition, Pearson Prentice Hall, Upper Saddle River, NJ, USA (2004).
[35] Y. P. Xiong, J. T. Xing and W. G. Price, Power flow analysis of complex coupled systems by progressive approaches, *Journal of Sound and Vibration*, 239 (2) (2001) 275-295.
[36] H. L. Sun, K. Zhang, P. Q. Zhang and H. B. Chen, Application of dynamic vibration absorbers in floating raft system, *Applied Acoustics*, 71 (3) (2010) 250-257.

Xinglong Gong received his doctorate degree in both experimental mechanics and optical measurement mechanics from the University of Science and Technology of China and the Saitama University in 1996, respectively. He is currently a professor in the University of Science and Technology of China. His current interests include intelligent material, vibration control, and mechanical design.

Chao Peng received his bachelor degree in mechanics engineering from Hefei University of Technology in 2004. He is currently a Ph.D student at the University of Science and Technology of China. His main research interests are vibration control and mechanical design.